Dielectric Properties of Poly(vinylidene fluoride) from Molecular Dynamics Simulations

Naoki Karasawa and William A. Goddard, III*

Materials and Process Simulation Center, Beckman Institute (139-74), Division of Chemistry and Chemical Engineering (CN 9009), California Institute of Technology, Pasadena, California 91125

Received November 1, 1994; Revised Manuscript Received June 13, 1995®

ABSTRACT: Molecular dynamics (MD) simulations at 300 and 400 K were used to calculate dielectric constants and dielectric loss for crystalline and amorphous poly(vinylidene fluoride). These calculations used the MSXX force field derived from first principles and tested previously for crystalline PVDF. In agreement with experiment the calculations lead to a dielectric constant of $\epsilon_0 = 8-13$ for amorphous PVDF but $\epsilon_0 = 2-3$ for crystalline PVDF. We show that the high ϵ_0 for amorphous PVDF arises from rapid changes in the torsion angles (and hence rapid modulation of the dipole moment perpendicular to the chain axis) during MD. These changes are enhanced by soliton-like defects in the chain that diffuse during the MD. The dielectric losses lead initially to a stretched exponential decay function, $\Phi(t) = \exp[-(t/\tau)^{\beta}]$, with $\tau = 60$ ps and $\beta = 0.62$ at 300 K.

1.0. Introduction

Previously, we developed[1] first principle force fields (MSXX and MSXXS) for poly(vinylidene fluoride), PVDF, and used them to predict the elastic constants, dielectric constants, and piezoelectric constants for crystalline PVDF. In this paper we predict the dielectric properties from the dipole moment autocorrelation function derived from molecular dynamics (MD).

Of particular interest is the large difference between the observed (static) dielectric constant for amorphous PVDF versus crystalline PVDF ($\epsilon_{amor} = 8-13$ versus $\epsilon_{xtl} = 2.2-3.5$).[2] For most other polymers the ratio is 1.5 or less. To learn the atomistic origin of this large difference, we carried out MD studies on both the crystalline and amorphous PVDF polymers. Section 2 summarizes the theory on which the analysis is based and provides other calculational details. The results of the calculations are presented in section 3, and the interpretations of the results are given in section 4.

2.0. Dielectric Loss and Dipole Moment Autocorrelations

The complex dielectric constant can be written as

$$\epsilon = \epsilon_1 - i\epsilon_2$$

where the real part ϵ_1 is in phase with the applied field and ϵ_2 leads to losses.

For an isotropic system the frequency dependent dielectric constant is given by[3c,4,5]

$$\frac{\epsilon(\omega) - \epsilon_\infty}{\epsilon_0 - \epsilon_\infty} = 1 - i\omega \int_0^\infty e^{-i\omega t}\Phi(t)\, dt \qquad (1)$$

where

$$\Phi(t) = \frac{(\langle \vec{M}(0)\cdot\vec{M}(t)\rangle - \langle \vec{M}\rangle^2)}{\langle \Delta M^2\rangle} \qquad (2)$$

Table 1. Dielectric Tensor Components for Crystalline PVDF II_{ad}

	ϵ_0			ϵ_∞
	MD	static		static
	no shell	no shell	with shell	with shell
ϵ_{xx}	1.19	1.22	2.23	1.90
ϵ_{yy}	1.33	1.19	2.14	1.83
ϵ_{zz}	1.13	1.14	2.16	1.87
ϵ_{xy}	−0.00	0	0	0
ϵ_{yz}	−0.00	0	0	0
ϵ_{xz}	−0.05	−0.07	−0.14	−0.02
$^1/_3(\epsilon_{xx} + \epsilon_{yy} + \epsilon_{zz})$	1.22	1.18	2.18	1.87

is the dielectric decay function and

$$\langle \Delta M^2\rangle = (\langle M^2\rangle - \langle \vec{M}\rangle^2) \qquad (3a)$$

is the total dipole moment fluctuation. Here the dipole function is

$$M_\alpha = \sum_I \mu_{\alpha I} \qquad (3b)$$

where the sum is over all atoms of the unit cell used in the MD simulations. The static dielectric constant is then given by the fluctuation formula,[3]

$$\epsilon_0 - \epsilon_\infty = \frac{4\pi\langle \Delta M^2\rangle}{3\Omega k_B T} \qquad (4a)$$

Here k_B is the Boltzmann constant, T is the temperature, and Ω is the volume of the cell. These formulas are derived from linear response theory using the canonical ensemble.[4]

In (4a), we assume the Ewald boundary condition in the simulations with a large real space cutoff length. Newmann and Steinhauser showed[3b] that the dielectric constant, ϵ_0, obtained from (4a) using dynamics with the Ewald boundary condition must be modified to

$$\epsilon_0^{\text{correct}} = \frac{(Q+2)(\epsilon_0 - 1) + 3}{(Q-1)(\epsilon_0 - 1) + 3} \qquad (4b)$$

* To whom correspondence should be addressed.

® Abstract published in *Advance ACS Abstracts,* September 1, 1995.

0024-9297/95/2228-6765$09.00/0

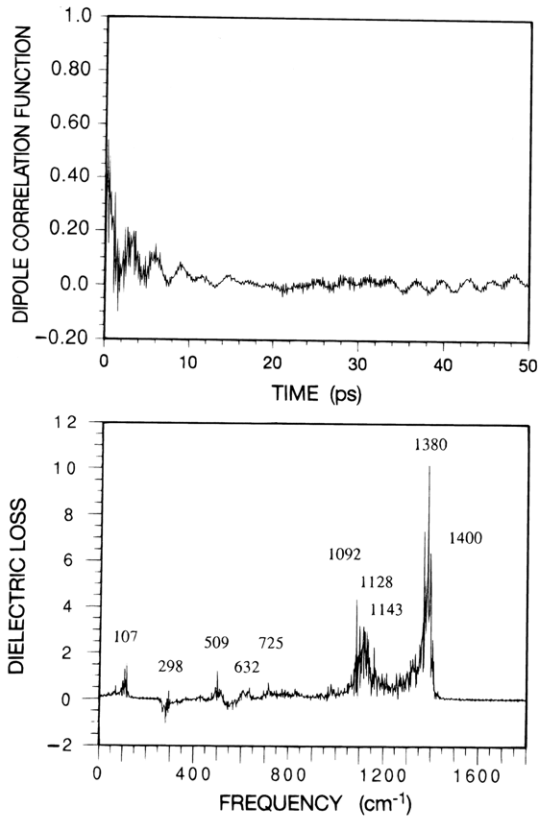

Figure 1. (a) Total dipole correlation functions of PVDF crystal form II_{ad} at $T = 300$ K. The initial 25 ps of dynamics was excluded so that a total 100 ps of dynamics ($t = 25$ ps to $t = 125$ ps) was used to obtain properties. (b) Imaginary part of the Fourier transform of the total dipole correlation function of PVDF form II_{ad} crystal at $T = 300$ K. Infrared frequencies calculated in ref 2 are also shown.

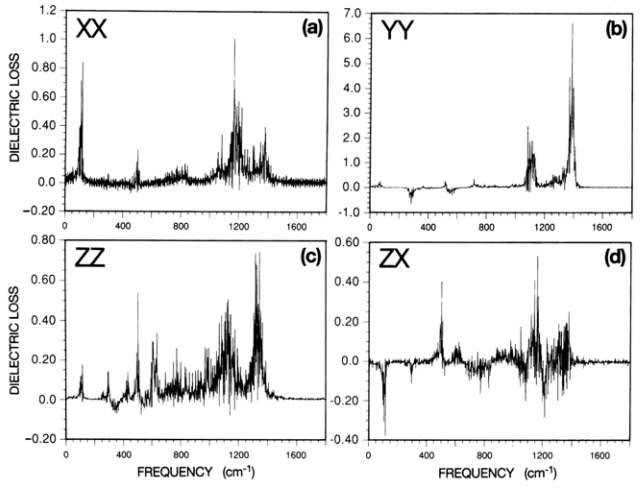

Figure 2. Imaginary part of the Fourier transforms of various compounds of the dipole correlation functions of PVDF form II_{ad} crystal at $T = 300$ K: (a) *XX*, (b) *YY*, (c) *ZZ*, and (d) *ZX*.

where Q is determined by the real space cutoff distance r_c,

$$Q = \int_0^{r_c} 4\pi r^2 \, dr \left(\frac{\eta}{\sqrt{\pi}}\right)^3 e^{-\eta^2 r^2} = \mathrm{erf}(\eta r_c) - \frac{2}{\sqrt{\pi}} \eta r_c e^{-\eta^2 r_c^2} \tag{4c}$$

where η is the Ewald parameter. For a large r_c, Q is close to 1 and $\epsilon_0^{\text{correct}} \sim \epsilon_0$. We use the reduced cell multipole method (RCMM),[6] where the long-range interactions are calculated using the Ewald procedure for a reduced set of atoms representing the unit cell moments. The cutoff distance for the real space summation is chosen such that adjustments of the final dielectric constants are very small. In our calculations, $Q = 0.999\,994$, leading to a change in ϵ_0 of 1.6×10^{-4}

Table 2. Dielectric Constants for Amorphous PVDF Calculated from Molecular Dynamics

(a) Canonical Dynamics at $T = 300$ K[a]

time (ps)	steps	ϵ_0 infinite chain	ϵ_0 finite chain
200	2000	3.64	7.02
300	3000	6.88	10.94
400	4000	8.48	12.23
500	5000	9.52	
600	6000	10.11	
700	7000	10.43	
800	8000	10.20	
900	9000	9.71	

(b) $T = 400$ K, Infinite Chain[b]

time (ps)	steps	ϵ_0 canonical	ϵ_0 microcanonical
40	2000	7.67	1.54
60	3000	8.89	1.53
80	4000	9.70	1.53
100	5000	10.97	1.54
120	6000	11.00	
140	7000	12.12	
160	8000	13.80	
180	9000	13.68	
200	10000	12.81	
220	11000	12.60	
240	12000	12.47	

[a] The initial 100 ps were skipped in calculating the dielectric constants. Thus the times used below correspond to $t = 100-1000$ ps. [b] The initial 100 ps were skipped in calculating the dielectric constant. Thus the times used below correspond to $t = 100-340$ ps.

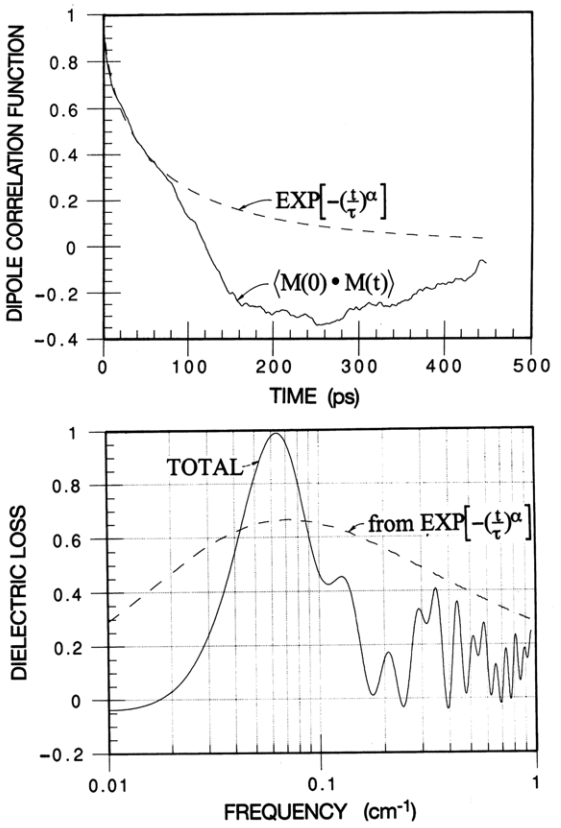

Figure 3. (a) Total dipole correlation function of amorphous PVDF at $T = 300$ K (based on the dynamics from $t = 100$ ps to $t = 1000$ ps). (b) Imaginary part of the Fourier transform of the total dipole correlation function.

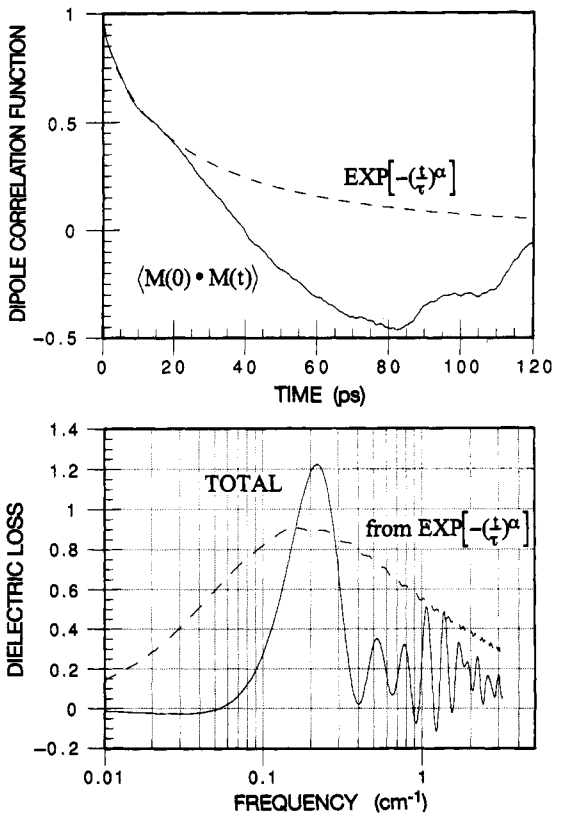

Figure 4. (a) Total dipole correlation function of amorphous PVDF at $T = 400$ K (based on the dynamics from $t = 100$ ps to $t = 340$ ps). (b) Imaginary part of the Fourier transform of the total dipole correlation function.

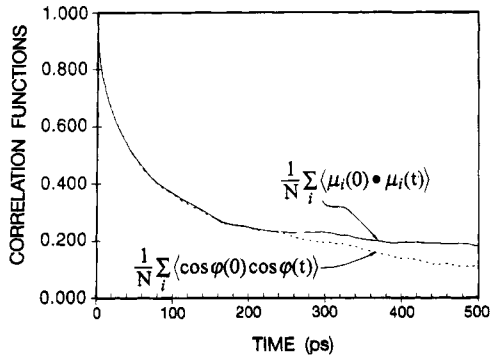

Figure 5. Monomer dipole correlation function $m(t)$ and torsional angle correlation function of amorphous PVDF at $T = 300$ K. This is based on the dynamics from $t = 100$ ps to 1100 ps.

for amorphous PVDF. Consequently, we neglected this correction.

For crystalline cases (1) can be generalized to[4]

$$\epsilon_{\alpha\beta}(\omega) = \epsilon_{0\alpha\beta} - \frac{4\pi}{\Omega k_B T} i\omega \int_0^\infty e^{-i\omega t} \mathscr{M}_{\alpha\beta}(t)\, dt \qquad (5)$$

where

$$\mathscr{M}_{\alpha\beta}(t) = \langle M_\alpha(0) M_\beta(t)\rangle - \langle M_\alpha\rangle\langle M_\beta\rangle \qquad (6)$$

The static dielectric tensor is

$$\epsilon_{0\alpha\beta} = \epsilon_{\infty\alpha\beta} + \frac{4\pi}{\Omega k_B T} \mathscr{M}_{\alpha\beta} \qquad (7)$$

where $\mathscr{M}$ is the variance tensor with components

$$\mathscr{M}_{\alpha\beta} = \langle M_\alpha M_\beta\rangle - \langle M_\alpha\rangle\langle M_\beta\rangle \qquad (8)$$

To evaluate these properties, we used canonical molecular dynamics[7,8] (Nosé with constant volume) with the MSXX force field.[1] This force field does *not* include the covalent shell model of the MSXXS FF and hence does not account for atomic polarizabilities. We showed earlier[1] that for crystals this underestimates ϵ_0 by ~1. However, use of the finite mass shell particle requires much shorter time steps ($\tau_{step} \sim 10^{-18}$ s instead of 10^{-15} s) while zero mass shell particles require evaluation of second derivatives. [An alternative approach for including shell dynamics is the quantum shell model.[9]]

In these simulations, the nonbond interactions (Coulomb and van der Waals) were calculated using the reduced cell multipole method (RCMM)[6] (second-order multipoles and second-order far-field expansions) with far-field updating every 10 steps. For 396 atoms per unit cell, RCMM is about 4 times faster than the Ewald method (accuracy of 0.01 kcal/mol per atom[10]) for similar total energy fluctuations.

The crystal calculations used a $2 \times 4 \times 2$ super cell (768 atoms) for the form II_{ad} crystal.[1]

The initial structure for the amorphous polymer was built using Monte Carlo procedures for 66 monomers (396 atoms), using periodic boundary conditions to eliminate surface effects. We used the experimental density ($\rho = 1.74$ g/cm^3) for 300 K and also used $\rho = 1.74$ g/cm^3 for 400 K. With only 396 atoms, the resulting molecular weight is small, and we were concerned that the ends of the finite chain would lead to an artificially high ϵ_0. In order to eliminate such end effects we grew a number of structures until we found ones whose termini were at nearly equivalent positions in different unit cells. We then connected these ends to obtain an infinite length chain.

In calculating the Fourier transforms in (1), we took the finite time simulation, e.g. a total of 1000 ps, truncated the initial relaxation portion (100 ps for amorphous 300 K), and calculated the dipole moment autocorrelation function using the remaining 900 ps of dynamics to form a periodic function for the Fourier transform (calculated using the method of Filon[11]). The maximum time for the correlation function is half of the simulation time (450 ps for 300 K). We used the trajectory every 0.1 ps, leading to 9000 steps. For amorphous PVDF at 400 K, we truncated the initial 100 ps and used the trajectory every 0.02 ps for next 120 ps, leading to 12 000 steps.

3.0. Results

3.1. Crystal PVDF (II_{ad}). The Nosé dynamics were equilibrated for 25 ps followed by measurements for an additional 50 ps. Using a snapshot of the geometry every 0.01 ps, we calculated the dipole fluctuations at 300 K. This leads to the results in Table 1.

In ref 1, ϵ_0 (300 K) was calculated using the vibrational modes (harmonic approximation), Table 1. Here we see an RMS difference of 0.07, indicating a close correspondence for the static and dynamical calculations. However, the dynamic values are about 1.0 smaller than observed with the MSXXS FF, indicating that the atomic polarization is important.

The total dipole correlation functions (eq 2) are shown in Figure 1a, while the frequency dependent dielectric loss is shown in Figure 1b. Here we see peaks corresponding to the infrared absorption bands.[1] Since we sampled the trajectory every 0.01 ps, the highest frequency is 1667 cm^{-1}. The infrared frequencies indicated in Figure 1b are from ref 1.

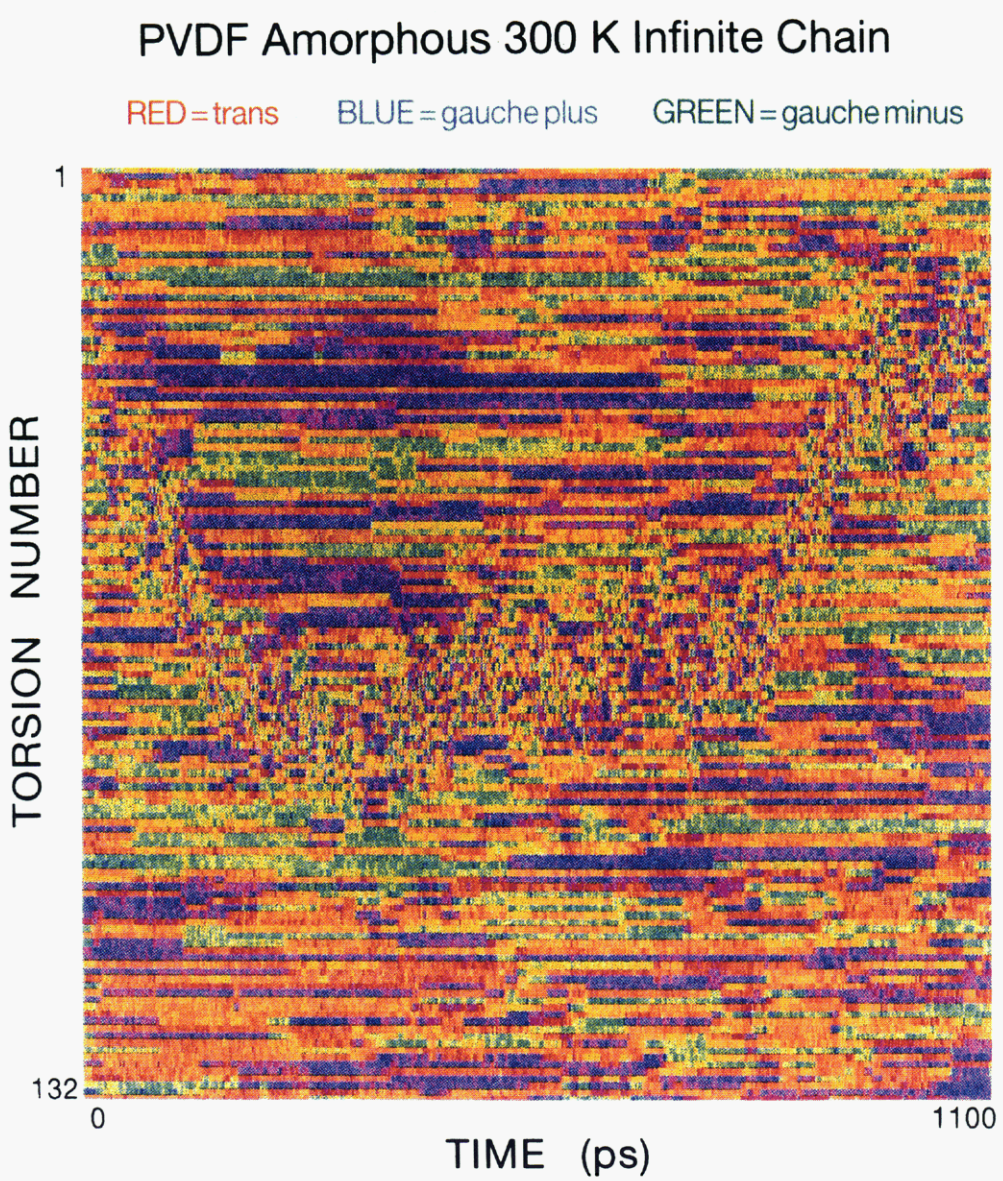

Figure 6. Torsional angles (color-coded) versus time for 1100 ps of canonical MD for the infinite chain system at $T = 300$ K.

For each component (*XX*, *YY*, *ZZ*, and *ZX*) of the dielectric constant, the frequency dependent dielectric loss is shown in Figure 2. This corresponds to the loss in electric energy in the system as a function of frequency. Since the dipole moment of the system couples to the external electric field, vibrational modes having a change in the dipole show up as peaks. The negative peaks for the *ZX* components arise from modes having changes in the dipole moments in the *X* and *Z* directions that are correlated and out of phase.

3.2. Amorphous PVDF. Canonical molecular dynamics calculations were performed for *infinite* chain systems at $T = 300$ K and at $T = 400$ K. The experimental values[12] at $\omega = 60$ Hz are 8.4−13.5 for 300 K, in reasonable agreement with the calculated values. Using (4), with the trajectory from 100 to 1000 ps (every 0.01 ps leading to 9000 steps), we obtain $\epsilon = 9.7$ at 300 K. Using (4) with the trajectory from 100 to 340 ps (every 0.02 ps, leading to 12 000 points), we obtain $\epsilon = 12.5$ at 400 K. From Table 2, we see that the dielectric constants converge in about 600 ps for $T = 300$ K and in about 140 ps for $T = 400$ K.

For canonical molecular dynamics with *finite* chain systems at 300 K, we find ϵ to be about 50% larger than for infinite chains (due to the flexibility of the chain ends), as indicated in Table 2a.

We also carried out microcanonical MD with an infinite chain system (Table 2b). Here the velocities of the atoms were scaled such that the average kinetic energy corresponds to a temperature of 400 K. This was done by first minimizing the energy of the system and then assigning a Gaussian velocity distribution corresponding to twice the bath temperature. When microcanonical dynamics are used, the torsional transitions are much less frequent (see Figure 9), leading to a dielectric constant of $\epsilon \sim 1.5$, much smaller than for canonical dynamics. This is consistent with previous studies[8b] which showed for polyethylene that microcanonical MD can take 100 times as long to equilibrate as canonical MD (for rotational barriers of ~2.5 kcal/mol). Thus we consider that the microcanonical calculation is not converged in the time of these calculations but the canonical MD is converged.

The total dipole moment correlation functions are shown in Figures 3a and 4a. For short times the dipole correlation functions are well fitted with the WW (Williams−Watts) stretched exponential function[13]

$$\Phi(t) = \exp\left[-\left(\frac{t}{\tau}\right)^{\alpha}\right] \tag{9}$$

The WW function is often used[13] to describe the relaxation behavior of amorphous polymers, leading usually

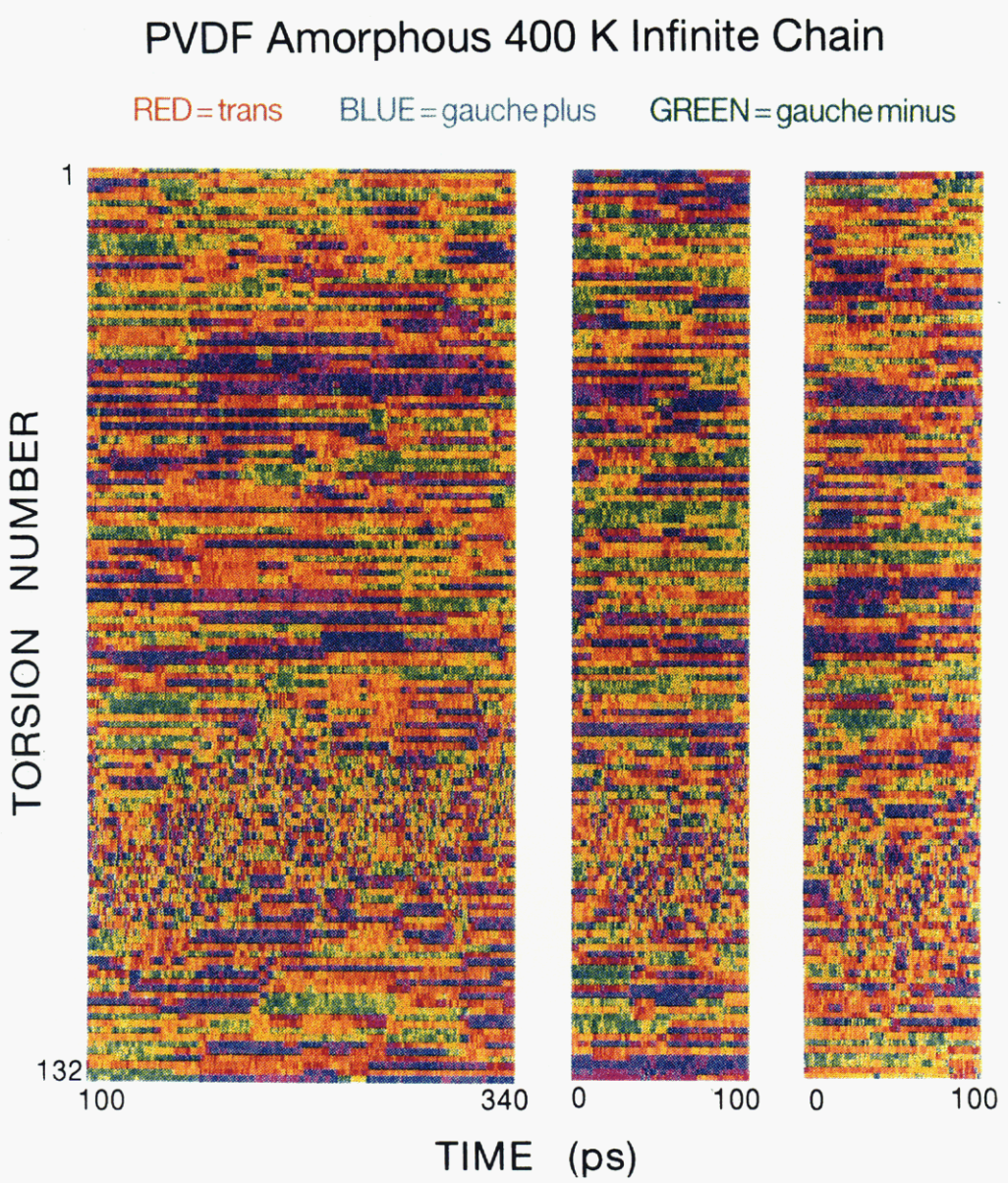

Figure 7. Torsional angles (color-coded) versus time for 240 ps of canonical MD for the infinite chain system at $T = 400$ K. Two independent runs for 100 ps starting from different initial structures are also shown.

to $\alpha \approx 0.5$. From the initial 80 ps of dynamics at $T = 300$ K, we obtain $\alpha = 0.618$ and $\tau = 59.5$ ps. Using the initial 20 ps at $T = 400$ K, we obtain $\alpha = 0.682$ and $\tau = 24.0$ ps. These fitted functions are shown in Figures 3 and 4.

In Figures 3a and 4a we see that the decay function goes negative for $t \sim 130$ ps at $T = 300$ K and for $t \sim 40$ ps at $T = 400$ K. This may be an artifact of the small size of the unit cell. It might also be due to the presence of only one independent chain per cell in these calculations.

The frequency dependent dielectric losses are plotted in Figures 3b and 4b and compared with the dielectric loss expected from the WW function. At 300 K the peak frequency in the dielectric loss is at 0.06 cm^{-1}, whereas at 400 K, the peak frequency moves to 0.2 cm^{-1}. Such increases in peak frequency with temperature are consistent with experiment.[14]

4.0. Interpretation

Theory and experiment agree that $\epsilon_{amor} \gg \epsilon_{xtl}$. The question is, why does the amorphous system lead to such a high dielectric constant? The dipole autocorrelation function for each monomer,

$$\frac{\sum_i \langle \vec{\mu}_i(0) \cdot \vec{\mu}_i(t) \rangle}{\sum_i \langle \mu_i^2(0) \rangle}$$

and the torsion correlation function,

$$\frac{\sum_i \langle \cos \phi_i(0) \cos \phi_i(t) \rangle}{\sum_i \langle \cos^2 \phi_i(0) \rangle}$$

are shown in Figure 5. This shows that in the amorphous phase the torsional angles change rapidly at $T = 300$ K. Since a monomer of PVDF has the dipole perpendicular to the chain axis, changes in the torsional angle modify the dipole moments, leading to a large dielectric constant for amorphous PVDF.

In searching for the origin of the larger ϵ_{amor}, we analyzed the torsional angle changes during the MD.

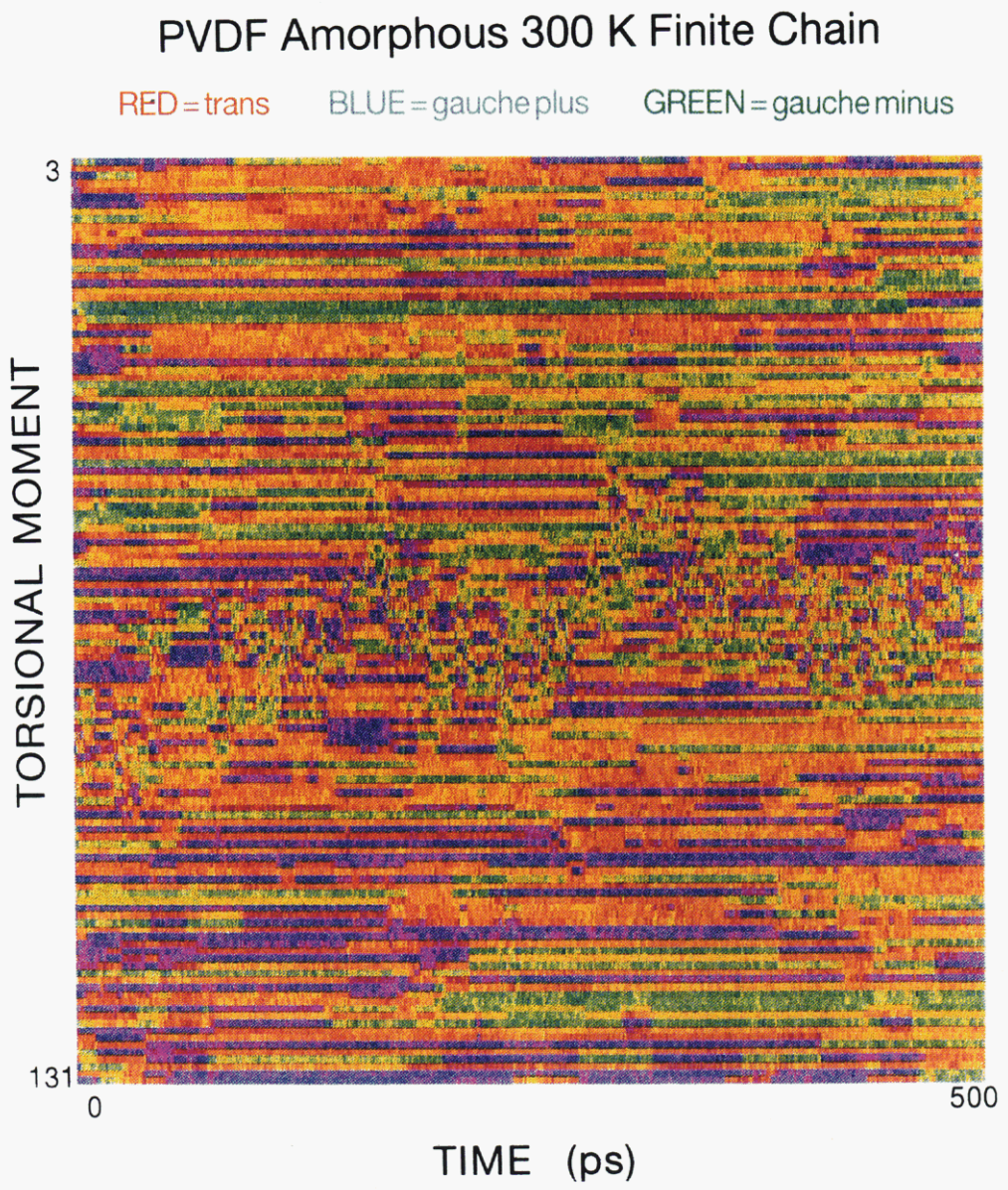

Figure 8. Torsional angles (color-coded) versus time for 500 ps of canonical MD of the finite chain system at $T = 300$ K.

The torsional angles are color-coded and plotted as functions of time in Figures 6–9. In these figures, all skeletal C–C–C–C torsional angles (1–132 for the infinite chain system) are shown by using three colors with intensities

$$I_R = \frac{1}{2}[\cos(\phi - \pi) + 1]$$

$$I_B = \frac{1}{2}\left[\cos\left(\phi - \frac{\pi}{3}\right) + 1\right]$$

$$I_G = \frac{1}{2}\left[\cos\left(\phi + \frac{\pi}{3}\right) + 1\right]$$

Thus, trans (T) is red, gauche plus (G^+) is blue, and gauche minus (G^-) is green. Other angles are shown by the combinations of these colors.

In Figure 6 we see that some torsional dihedral angles are unchanged during the full 1100 ps of dynamics while others change frequently. Indeed, we see a region about 30 atoms long which exhibits rapid fluctuations between T, G^+, and G^-. This region starts at around ϕ_{50} for $t =$ 100 ps, moves to near ϕ_{90} after 300 ps, and then back to ϕ_{30} by 1100 ps. We find that this system leads to a negative vibrational mode. Hence it is unstable but cannot relax without cutting the polymer and reconnecting. Thus we consider this entity to be a *soliton*. Figure 10 shows a stereoview of the soliton from $t =$ 100 ps ($T = 300$ K). The soliton moves between ϕ_{20} and ϕ_{90} with a period of about 900 ps. Apparently, the soliton configuration is compatible with atom positions in the ϕ_{20} to ϕ_{90} region but the structures at ϕ_{20} and ϕ_{90} cause a reflection. At 400 K the soliton moves faster, covering a larger region.

We generated infinite chain structures four times and finite chain structures twice. In all six cases a soliton was found. Since the dipole moment is perpendicular to the chain axis, we expect the soliton to have a dipole moment perpendicular to its axis. The easy migration of the soliton in the dynamics suggests an easy polarizability and hence a high ϵ. Thus we believe that the soliton explains the high ϵ for amorphous PVDF.

Various theoretical models have been used to explain the nonexponential decay behavior in the dielectric relaxation of amorphous polymers.[14–17] Our canonical molecular dynamics studies support defect diffusion models[15] and soliton models.[16] We regard the localized part of the chain where torsion angles change rapidly (shown in Figures 6–8) as a soliton-like defect of the chain that diffuses along the chain.

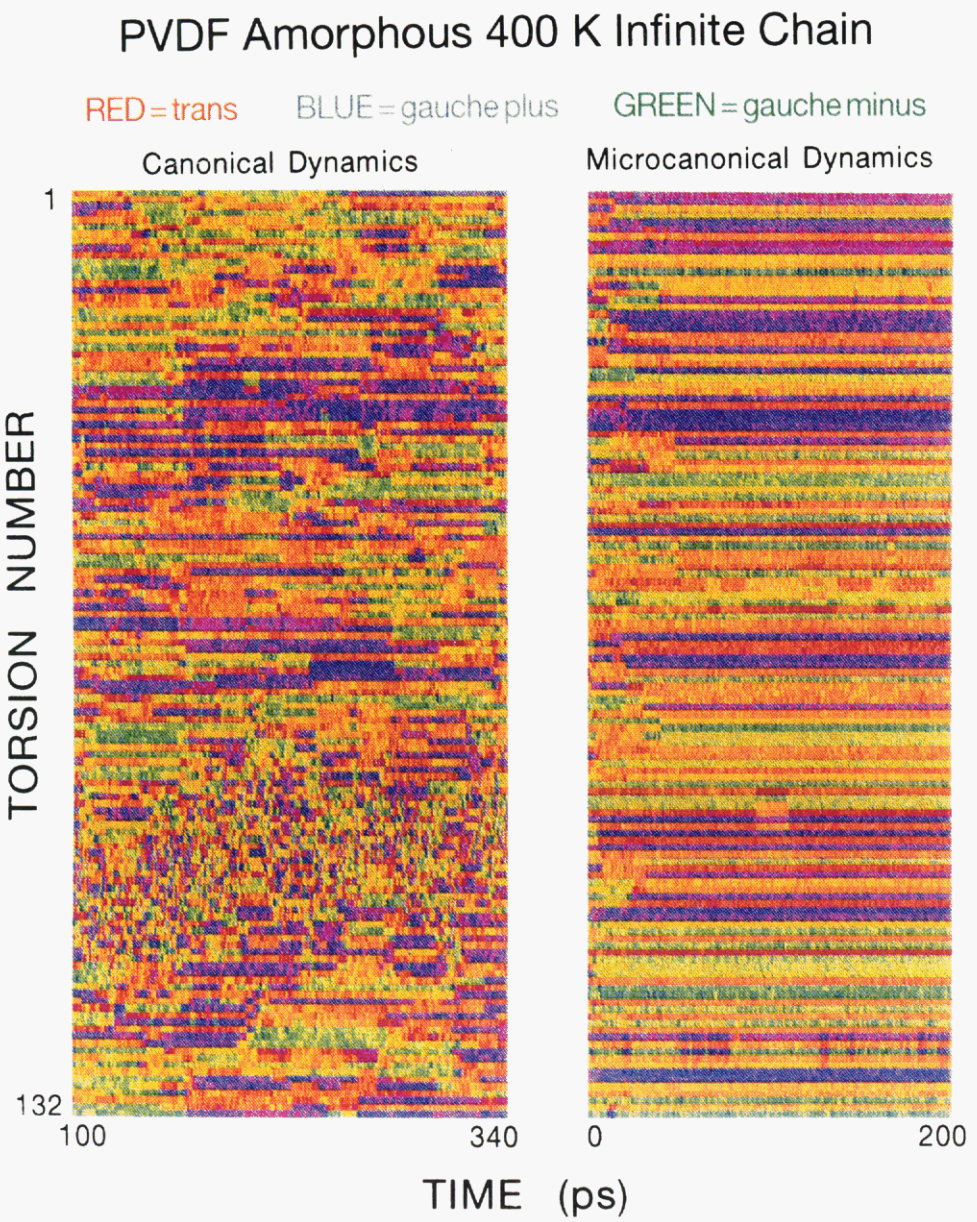

Figure 9. Comparison between canonical and microcanonical MD of the infinite chain system at $T = 400$ K.

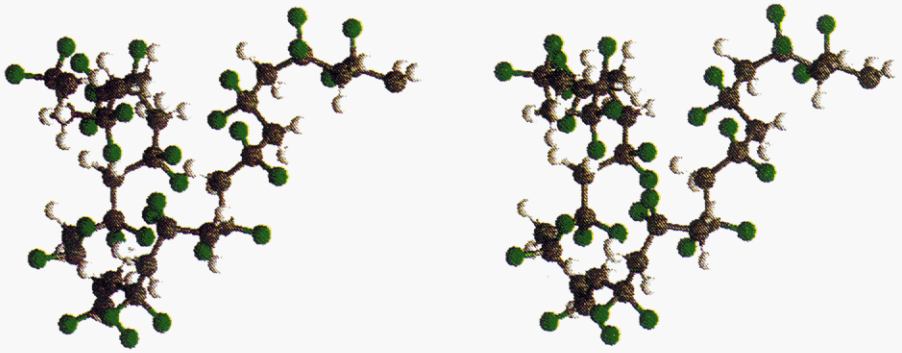

Figure 10. Stereoview of the soliton (30 carbon fragment) of the PVDF polymer chain from canonical molecular dynamics (infinite chain) at $T = 300$ K (100 ps point from Figure 5).

In the microcanonical dynamics, changes of conformation were quite rare and Figure 9 shows that the localized rapidly changing region (the soliton) was not observed in the 100 ps time scale.

5.0. Summary

Canonical MD calculations were performed on crystalline and amorphous PVDF polymers. For the crystal case the dielectric tensor from MD and from static calculations are in agreement with each other ($\epsilon_0 \sim 2-3$) and with experiment ($\epsilon_0 = 2.2-3.5$). The frequency response agrees with the infrared frequencies of the crystal.

For amorphous systems, the static dielectric constants were calculated to be much larger, $\epsilon_0 = 9.7$ ($T = 300$ K) and $\epsilon_0 = 12.5$ ($T = 400$ K), in agreement with experimental values ($\epsilon_0 = 8-13$). We found a localized soliton-like torsional defect that diffuses along the chain in the

amorphous system. The large dielectric constants are shown to arise from large changes of torsional angles of chains during dynamics. We associate these rapid changes with the soliton.

Acknowledgment. The research was funded by NSF (CHE 91-100289, ACR 92-17368, CHE 94-13930). The facilities of the MSC are also supported by grants from DOE-BCTR, Allied-Signal Corp., Aramco, Asahi Chemical, Asahi Glass, BP Chemical, Chevron Petroleum Technology Co., Oronite, BF Goodrich, Xerox, Hughes Research Laboratories, Hercules, Teijin Ltd., Vestar, and Beckman Institute. Some calculations were carried out on the NSF Pittsburgh supercomputer systems and on the JPL Cray.

References and Notes

(1) Karasawa, N.; Goddard, W. A., III. *Macromolecules* **1992**, *25*, 7268.
(2) Bicerano, J. *Predictions of Polymer Properties*; Marcel Dekker: New York, 1993.
(3) (a) Neumann, M. *Mol. Phys.* **1983**, *50*, 841. (b) Neumann, M.; Steinhauser, O. *Chem. Phys. Lett.* **1983**, *95*, 417. (c) Neumann, M.; Steinhauser, O. *Chem. Phys. Lett.* **1983**, *102*, 508.
(4) Kubo, R. *J. Phys. Soc. Jpn.* **1957**, *12*, 570.
(5) Fröhlich, H. *Theory of Dielectrics, Dielectric Constants and Dielectric Loss*; Oxford at Claredon Press: Oxford, U.K., 1958.
(6) Ding, H-Q.; Karasawa, N.; Goddard, W. A., III. *Chem. Phys. Lett.* **1992**, *196*, 1.
(7) Nosé, S. *J. Chem. Phys.* **1984**, *81*, 511.
(8) (a) Cagin, T.; Karasawa, N.; Dasgupta, S.; Goddard, W. A., III. *Mater. Res. Soc. Symp. Proc.* **1992**, *278*, 61. (b) Cagin, T.; Goddard, W. A., III; Ary, M. L. *Comput. Polym. Sci.* **1991**, *1*, 241.
(9) Kiang, C-H.; Goddard, W. A., III. *J. Chem. Phys.* **1993**, *98*, 1451.
(10) Karasawa, N.; Goddard, W. A., III. *J. Phys. Chem.* **1989**, *93*, 7320.
(11) Filon, L. N. G. *Proc. R. Soc. Edinburgh* **1928**, *A49*, 38.
(12) *Polymer Handbook*; Brandrup, J., Immergut, E. H., Eds.; John Wiley & Sons: New York, 1989; pp V/52.
(13) Williams, G.; Watts, D. C. *Trans. Faraday Soc.* **1970**, *66*, 80.
(14) Shore, J. E.; Zwanzig, R. *J. Chem. Phys.* **1975**, *63*, 5445.
(15) Bordewijk, P. *Chem. Phys. Lett.* **1975**, *32*, 592.
(16) Skinner, J. L.; Wolynes, P. *J. Chem. Phys.* **1980**, *73*, 4015.
(17) Skinner, J. L. *J. Chem. Phys.* **1983**, *79*, 1955.

MA946385L